

# Higgs Prospects at the Upgraded Tevatron: Fermilab Study Results

John D. Hobbs  
*SUNY – Stony Brook*

Preliminary results from a Fermilab study of the sensitivity for higgs production at the Tevatron in run II and beyond are presented. The study extends existing results by systematically combining results for all decay channels, considering the production of higher mass higgs bosons and interpreting the results in the context of supersymmetric higgs production as well as standard model production. In addition new analysis methods which significantly improve sensitivity are used.

## I. INTRODUCTION

The standard model of particle physics has been studied with very high precision over the course of the past ten years, and no significant deviations have been found. Despite this, our understanding of the origin of electroweak symmetry breaking is still incomplete. This arises in large part because the only remaining undetected standard model particle, the higgs boson, mediates electroweak symmetry breaking in the standard model. The highest available center-of-mass energy for the years 2000 to 2004 will be at the Fermilab Tevatron  $p\bar{p}$  collider with  $\sqrt{s} = 2.0$  TeV. It is natural to explore the sensitivity to higgs production at the Tevatron. This paper contains preliminary results from a year-long study conducted jointly by the Fermilab theory group and the CDF and DØ experiments. The goal is to quantify the higgs discovery potential at the Tevatron in the coming run II and possible extensions. Results are presented as the luminosities required to exclude higgs at the 95% confidence level, or to establish either  $3\sigma$  or  $5\sigma$  excesses over predicted backgrounds.

The starting points for this study are the higgs mass constraints expected from LEP2 [1] and previous Fermilab studies [2] [3]. This study extends the previous Fermilab results by (1) including additional standard model decays in the mass regions previously explored, (2) testing the sensitivity for higgs masses  $M_H > 135$  GeV, (3) systematically combining results from all channels, (4) interpreting the results as supersymmetric(SUSY) higgs production and (5) considering additional decay modes arising from SUSY models. In addition, a detector simulation was developed which gives significantly more realistic event reconstruction than some of the previous studies used.

This paper has six sections. The first describes the production and decay of standard model higgs bosons and the simulations used in this study. The second and third sections contain results for standard model higgs production in the mass ranges  $90 \leq M_H < 135$  GeV and  $135 < M_H < 200$  GeV respectively. The fourth section presents the combination of the results in sections two and three. The fifth section describes the extension of the results to SUSY production. The last section describes studies of additional SUSY-specific decays, particularly final states having four  $b$ -quarks.

## II. PRODUCTION, DECAY, EVENT GENERATION AND DETECTOR SIMULATION

The production cross sections [4] and decay branching ratios for a standard model higgs boson are shown in Fig. 1. These plots indicate that the highest cross section production modes are  $p\bar{p} \rightarrow H$ ,  $p\bar{p} \rightarrow WH$  and  $p\bar{p} \rightarrow ZH$ . The higgs decays dominantly to the most massive kinematically allowed final state. For  $M_H < 135$  GeV, the dominant decay mode is  $H \rightarrow b\bar{b}$  with a branching ratio of roughly 80%. For  $M_H > 135$  GeV, the dominant mode is  $H \rightarrow WW$ . Thus, searches for lower-mass higgs will be looking for final states with at least two  $b$ -flavored jets, and the higher mass searches will have multiple (virtual)  $W$  bosons. For most of the mass range in question, the  $p\bar{p} \rightarrow H$  mode has very poor signal-to-noise, and the most useful modes are the  $p\bar{p} \rightarrow WH$  and  $p\bar{p} \rightarrow ZH$  modes with the  $W$  or  $Z$  decaying to leptons.

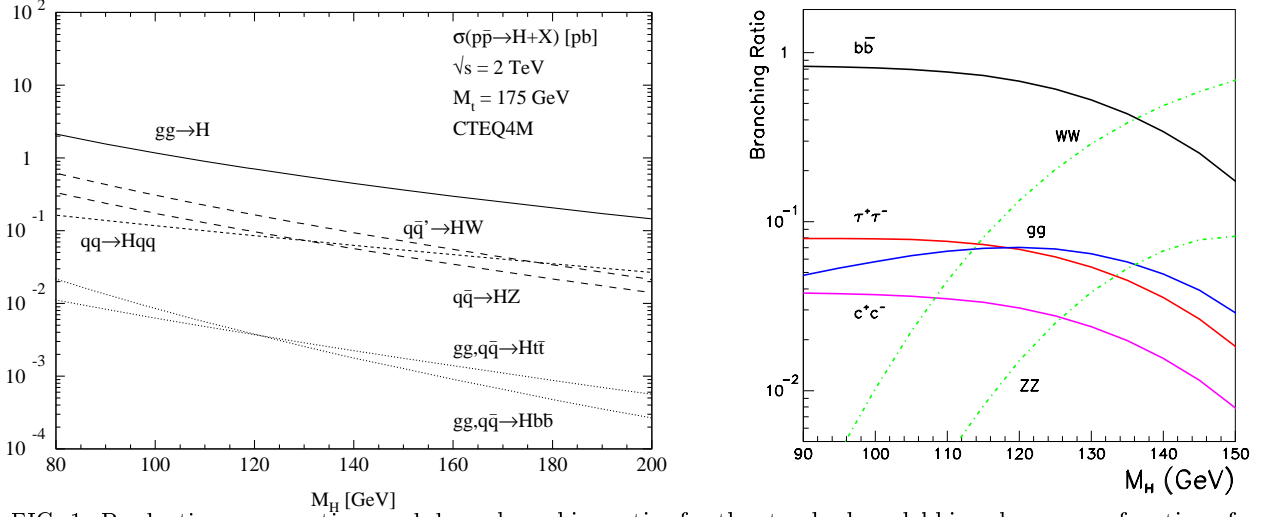


FIG. 1. Production cross sections and decay branching ratios for the standard model higgs boson as a function of mass.

Unless explicitly noted, events used in these analyses were generated using the Pythia [5], Isajet [6] or CompHep [7] programs. The generated four-vectors were then input to a detector simulation program, SHW, developed for the run II workshop [8]. This program uses parameterized resolutions for tracking and calorimeter systems and particle identification to perform simple reconstruction of tracks, calorimeter-based jets, vertices and trigger objects. The resolutions used represent a typical run II detector and are drawn from CDF and DØ internal studies. Particle identification efficiencies are included by parameterizing results from other CDF and DØ studies.

The SHW program was verified by comparing selection efficiencies between SHW and data or between SHW and well-established run I simulations used by CDF or DØ. The most stringent test was a comparison of nearly identical analyses of the  $p\bar{p} \rightarrow WH \rightarrow (\ell\nu)(b\bar{b})$  channel. Two analyses of this channel have been performed, one based on a run I CDF simulation with the geometrical acceptance extended to correspond to the run II CDF detector and the second based purely on SHW. The first analysis predicts 5.0 signal events and 62.8 background events/fb $^{-1}$  for  $M_H = 110$  GeV. The second predicts 4.5 signal and 62.5 background events for the same conditions.

### III. LOW MASS HIGGS SEARCHES, $M_H < 135$ GEV

When  $M_H < 135$  GeV, the dominant decay mode is  $H \rightarrow b\bar{b}$ . Analyses have been performed for all  $p\bar{p} \rightarrow WH$  and  $p\bar{p} \rightarrow ZH$  final states.<sup>1</sup> The possible final states are: (1)  $p\bar{p} \rightarrow WH \rightarrow \ell\nu b\bar{b}$ , (2)  $p\bar{p} \rightarrow ZH \rightarrow \nu\bar{\nu} b\bar{b}$ , (3)  $p\bar{p} \rightarrow ZH \rightarrow \ell^+\ell^- b\bar{b}$  and (4)  $p\bar{p} \rightarrow WH \rightarrow q\bar{q} b\bar{b}$  or  $p\bar{p} \rightarrow ZH \rightarrow q\bar{q} b\bar{b}$ . The primary backgrounds to these channels are  $W + b\bar{b}$  and  $Z + b\bar{b}$  with the  $b\bar{b}$  pair from gluon radiation, single top-quark production and top-quark pair production.

All analyses for these channels begin with a preliminary selection based on the number and type of final state objects. For example, the  $p\bar{p} \rightarrow WH \rightarrow \ell\nu b\bar{b}$  analysis requires a charged lepton with  $E_T > 20$  GeV, missing transverse energy  $\cancel{E}_T > 20$  GeV and two  $b$ -tagged jets having  $E_T > 15$  GeV. Similar selections are applied for the other channels. After the basic selection, a requirement is made that the mass of the reconstructed  $b\bar{b}$  system be within (typically)  $2\sigma$  of the generated higgs mass. Additional clean up requirements are also made. As an example, in the  $p\bar{p} \rightarrow ZH \rightarrow \nu\bar{\nu} b\bar{b}$  channel, there can be no isolated tracks with  $p_T > 15$  GeV. This rejects events with high- $p_T$  leptons which failed the lepton identification. The resulting number of signal and background events corresponding to 1 fb $^{-1}$  of data are given

<sup>1</sup>The mode  $p\bar{p} \rightarrow H \rightarrow b\bar{b}$  was considered, but the signal to noise was too poor for it to have any sensitivity when compared to the  $p\bar{p} \rightarrow WH$  and  $p\bar{p} \rightarrow ZH$  modes.

in table I. The  $p\bar{p} \rightarrow WH \rightarrow \ell\nu b\bar{b}$  and  $p\bar{p} \rightarrow ZH \rightarrow \nu\bar{\nu} b\bar{b}$  modes offer the best sensitivity with the  $p\bar{p} \rightarrow ZH \rightarrow \ell^+\ell^- b\bar{b}$  mode not far behind. The all-hadronic final state looks quite difficult.

In addition to these analyses, a multivariate analysis using neural networks has been performed for the  $p\bar{p} \rightarrow WH \rightarrow \ell\nu b\bar{b}$  channel. This style of analysis has been used with considerable success by DØ in the top mass [9] and all-hadronic top decay analyses. [10] The basic principle is to exploit correlations within an event in an automatic manner. The left panel of Fig. 2 shows the number of predicted signal and background events for  $p\bar{p} \rightarrow WH \rightarrow \ell\nu b\bar{b}$  analyses. Each point in the figure represents one possible analysis. The band labelled “rgsearch” corresponds to hypothetical analyses performed using selections using the standard technique of sequential requirements applied to event variables, with each requirement a single-valued comparison such as  $\cancel{E}_T > 20$  GeV. The point labelled “TeV 2000” is the result from a previous Fermilab study [2]. The point labelled “neural net” is the result from the multivariate analysis. One sees that for a fixed background, the signal is increased by roughly 50% using the neural network. Similar gains are expected in all other channels in this mass range.

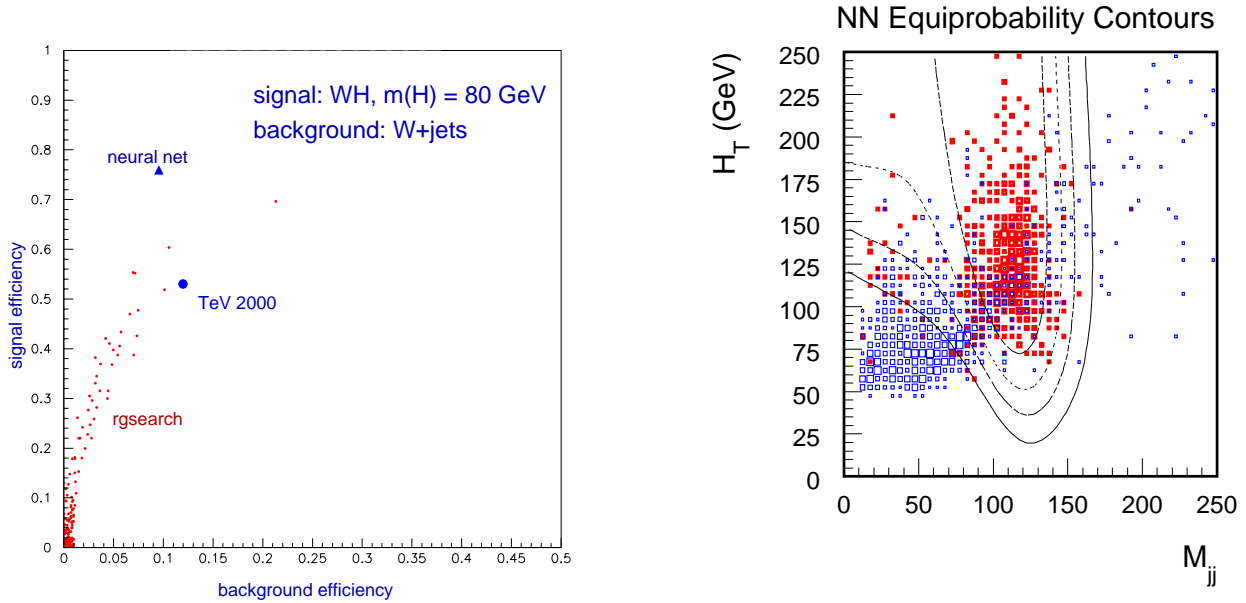


FIG. 2. The left panel shows predicted signal and background selection efficiencies from the neural network analysis. Each point corresponds to a possible event selection. The point labelled “neural net” is the result from the multivariate analysis described in the text. The right panel shows neural network output equal probability contours in the  $H_T$  vs.  $M_{jj}$  plane.  $H_T$  is the scalar sum of all jet energies, and  $M_{jj}$  is the invariant mass of the tagged dijet system. The open boxes are background events, and the closed boxes are signal.

### A. Other Improvements

Results have also been obtained for hypothetical improvements in mass reconstruction and  $b$ -jet tagging efficiency. The analyses were repeated after artificially improving the reconstructed dijet mass resolution in steps up to a 50% better resolution. The results in Tab. I include an improvement in mass resolution of 30%. This level of improvement is possible when information such as charged track energy is used in the mass reconstruction in association with the calorimeter-based jet energies currently used. Such an improvement has already been realized in a preliminary run I CDF analysis of the  $p\bar{p} \rightarrow Z \rightarrow b\bar{b}$  channel. [11] Improved mass resolution offers considerable benefits because for a selection with a fixed signal expectation, the background will decrease as the resolution improves.

The effect of improved  $b$ -jet tagging has also been explored by artificially improving the second jet tagging efficiency by up to a factor of two. The gains from this improvement are not as important as those from mass resolution improvements because both signal and background increase with improved tagging efficiency.

#### IV. HIGH MASS HIGGS SEARCHES, $M_H > 135$ GEV

Previous Fermilab studies have concentrated on the lower mass higgs states which decay dominantly to  $b\bar{b}$ . This study includes analyses designed for final states in which the higgs decays to  $WW$  or  $ZZ$  instead of  $b\bar{b}$ . This corresponds approximately to  $M_H > 135$  GeV. Three final states are considered: (1) Three leptons,  $l^\pm l'^\pm l^\mp$ , arising primarily from  $p\bar{p} \rightarrow WH \rightarrow WWW$ , (2) Dileptons and neutrinos,  $l^+ l^- \nu \bar{\nu}$ , from  $p\bar{p} \rightarrow H \rightarrow WW$  and (3) Like-sign dileptons plus jets,  $l^\pm l^\mp jj$ , from  $p\bar{p} \rightarrow WH \rightarrow WWW$  and  $p\bar{p} \rightarrow ZH \rightarrow ZWW$ . [12] The dominant backgrounds are standard model production of  $WW$ ,  $WZ$ ,  $ZZ$ , and  $W(Z) + jets$  and  $t\bar{t}$  and multijet events with misidentification arising from detector effects. The standard model sources dominate the detector effects.<sup>2</sup>

As for the low mass analyses, the initial selections are based on simple variables related to the boson decay-product kinematics. However, to reach usable sensitivity, the analyses then use either (1) requirements typically relating to angular correlations arising from spin differences between signal and background or (b) likelihood methods. In both cases new variables have been designed. Figure 3 shows one such variable used in the  $l^+ l^- \nu \bar{\nu}$  analysis, the cluster mass  $M_C \equiv \sqrt{p_T^2(\ell\ell) + m^2(\ell\ell)} + \cancel{E}_T$ . A result of the tuning is that the signal and background have similar mass distributions, so these analyses must be treated as straight counting experiments. The numbers of expected signal and background events for the high-mass channels are given in table II.

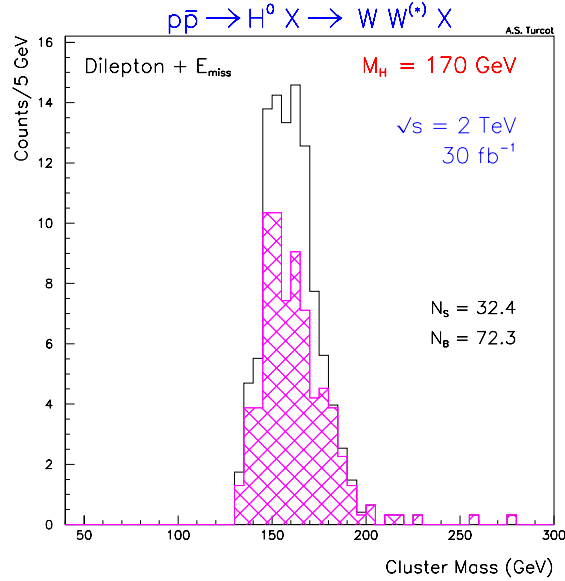


FIG. 3. The cluster mass variable for background (shaded region) and for signal and background together (open region) for the  $l^+ l^- \nu \bar{\nu}$  analysis.

#### V. COMBINATION OF STANDARD MODEL SEARCH CHANNELS

The results in the preceeding two sections have also been combined to form a single unified result. Figure 4 shows the luminosities required for 95% CL exclusion,  $3\sigma$  evidence and  $5\sigma$  discovery as a function of standard model higgs mass. These contours include statistical and systematic errors<sup>3</sup> and the channels are combined using the prescription of reference [13].

<sup>2</sup>In general, the backgrounds arising from detector effects use conservative misidentification probabilities based on run I analyses by both experiments.

<sup>3</sup>The systematic errors are assumed to scale with luminosity. The scaling is expected to hold at least until 2% relative systematic errors are reached. Systematic uncertainties at this level do not limit the analyses.

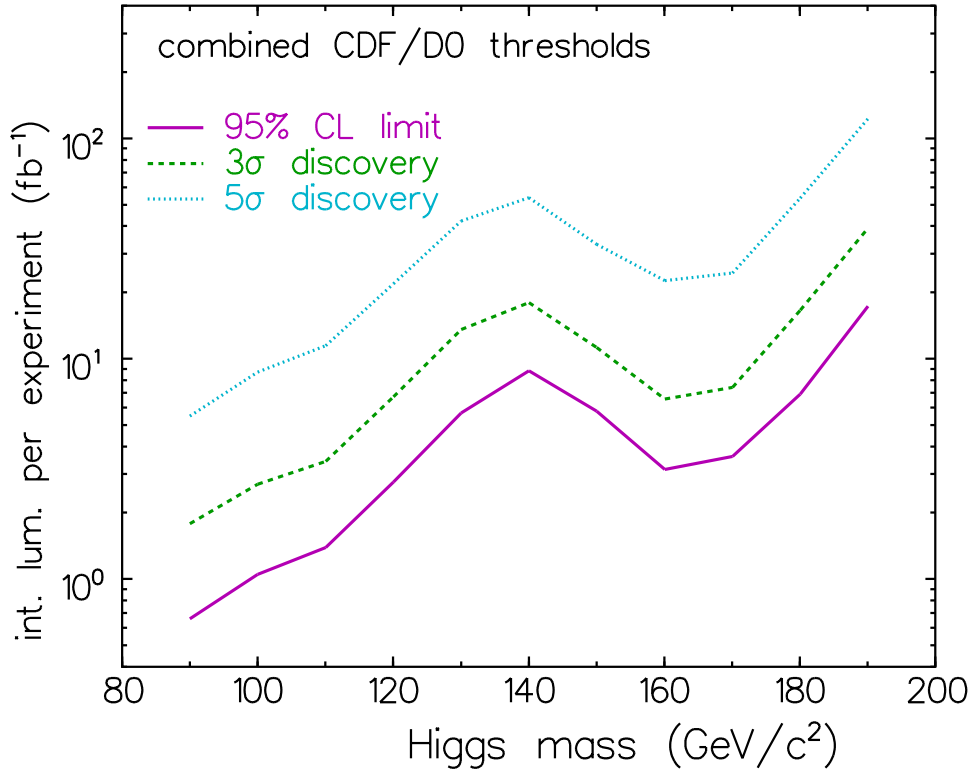


FIG. 4. Luminosity required to achieve 95% confidence level exclusion,  $3\sigma$  evidence and  $5\sigma$  discovery as a function of higgs mass. The results use all channels and assume results from both CDF and DØ having equal sensitivity. The experimental uncertainties used are described in the text.

## VI. SEARCH FOR NEUTRAL HIGGS BOSONS IN SUSY MODELS

Most supersymmetric extensions of the standard model result in five physical higgs states, two neutral scalars denoted  $h$  and  $H$  (with  $M_h < M_H$ ), a single pseudoscalar  $A$  and the charged doublet  $H^\pm$ . Unlike most other supersymmetric particles, the masses of the higgs particles depend only on two parameters, typically chosen to be  $\tan\beta$  and  $M_A$  (or  $M_h$ ). Furthermore, the  $h$  boson must satisfy  $M_h < 130$  GeV, and it may easily be less massive than this. For much of SUSY phase space, the  $h$  decay is identical to that of the standard model higgs, and only the production cross section differs. Given this, the searches for low mass standard model higgs can be easily converted to searches for SUSY higgs. The left-hand panel of Fig. 5 shows the  $5\sigma$  exclusion contour in the  $\tan\beta$  vs.  $M_A$  plane for the case in which all non-higgs SUSY masses are around 1 TeV, the systematic error is 10%, and CDF and DØ data are combined. One sees that for this example, SUSY models having  $1 < \tan\beta < 50$  and  $80 < M_A < 400$  GeV are excluded.

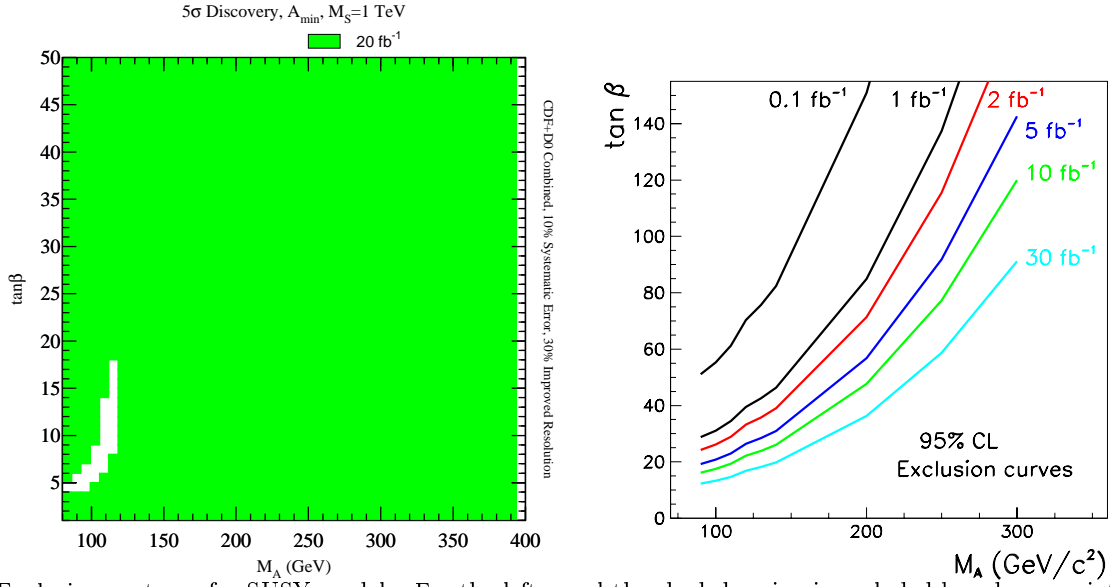


FIG. 5. Exclusion contours for SUSY models. For the left panel the shaded region is excluded based on a reinterpretation of the standard model searches in section two as SUSY higgs production. This example shows the  $5\sigma$  exclusion region with an integrated luminosity of  $20 \text{ fb}^{-1}$ . The right panel shows the result from the  $p\bar{p} \rightarrow \phi b\bar{b} \rightarrow b\bar{b}b\bar{b}$  analysis described in section VII.

## VII. SEARCHES FOR THE SUSY MODE $p\bar{p} \rightarrow \phi b\bar{b} \rightarrow b\bar{b}b\bar{b}$ , $\phi = H, A, H$

Within SUSY models, new higgs production modes exist, some with couplings proportional to  $\tan^2 \beta$ . For sufficiently large values of  $\tan\beta$  these become the dominant production modes. One such mode is  $p\bar{p} \rightarrow h b\bar{b}$ <sup>4</sup>. This results in final states containing four  $b$ -flavored jets. Analyses of this channel have been carried out. These typically require four jets, three of which satisfy  $b$ -tag requirements. All possible mass combinations of  $b$ -jets are computed, and the resulting distribution is examined for a peak near the generated higgs mass. The 95% C.L. exclusion contours in the  $\tan\beta$  vs.  $M_A$  plane are shown in the right panel of Fig. 5 for a variety of integrated luminosities.

## VIII. CONCLUSIONS

Studies of the experimental sensitivity to higgs production for Tevatron Run II and beyond have been carried out. Both standard model and supersymmetric higgs production have been considered. It is found that with  $4 \text{ fb}^{-1}$  of data, standard model higgs can be excluded at 95% confidence over the interval  $M_H < 125 \text{ GeV}$  and  $155 < M_H < 175 \text{ GeV}$ . With  $10 \text{ fb}^{-1}$ , a standard model higgs boson will be seen as at least a  $3\sigma$  excess over the mass ranges  $M_H < 125 \text{ GeV}$  and  $145 < M_H < 175 \text{ GeV}$ . These results have been converted to limits on the SUSY parameter space, with one example shown.

---

[1] *Prospects for the Higgs Boson Search in  $e^+e^-$  Collisions at LEP-200*, By the OPAL, Delphi, Aleph and L3 collaborations, CERN-EP-98-094.

---

<sup>4</sup>There are additional modes with  $A$  or  $H$  in place of  $h$ .

- [2] *Future Electroweak Physics at the Fermilab Tevatron, Report of the tev\_2000 Study Group*, Amidei and Brock, ed., FERMILAB-PUB-96/082.
- [3] The TeV33 Committee Report, Amidei, *et. al.*, <http://www-theory.fnal.gov/tev33.ps>
- [4] *Higgs Boson Production and Decay at the Tevatron*, M. Spira, hep-ph/9810289, and A. Djouadi, J. Kalinowski and M. Spira, hep-ph/9704448.
- [5] T. Sjostrand, Computer Physics Commun. 82 (1994) 74, and the Supersymmetric extensions in S. Mrenna, ANL-HEP-PR-96-63.
- [6] F. Paige and S. Protopopescu, BNL Report no. BNL38034, 1986 (unpublished).
- [7] A. S. Belyaev, A. V. Gladyshev, A. V. Semenov, hep-ph/9712303 and E. E. Boos *et. al.*, hep-ph/9503280.
- [8] <http://www.physics.rutgers.edu/~jconway/soft/shw/shw.html>, to appear in the *Report of the Fermilab Run II SUSY/Higgs working group*.
- [9] S. Abachi, *et. al.*, Phys. Rev. **D58** 052001 (1998), hep-ex/9801025.
- [10] S. Abachi, FERMILAB PUB-98/130-E, hep-ex/9808034, accepted for publication in Phys. Rev. **D**.
- [11] Tommaso Dorigo, *Search for Z decays to b Quark Pairs at the Tevatron pp Collider*, Ph.D. Thesis, University of Padova 02/99.
- [12] T. Han, A. S. Turcot and R. Zhang, Phys. Rev. **D59**, 093001 (1999), hep-ph/9812275
- [13] The statistics conventions are described <http://fnth37.fnal.gov/higgs/conv5.ps> and will appear in *Report of the Fermilab Run II SUSY/Higgs working group*.

TABLE I. Numbers of expected signal and background events for each low-mass channel in  $1 \text{ fb}^{-1}$ . A 30% improvement in mass resolution over that from SHW has been assumed. See the text for details.

Channel	Rate	Higgs Mass ( $\text{GeV}/c^{-1}$ )				
		90	100	110	120	130
$\nu\bar{\nu}b\bar{b}$	$S$	2.5	2.2	1.9	1.2	0.6
	$B$	10	9.3	8.0	6.5	4.8
	$S/\sqrt{B}$	0.8	0.7	0.7	0.5	0.3
$l\nu b\bar{b}$	$S$	8.4	6.6	5.0	3.7	2.2
	$B$	48	52	48	49	42
	$S/\sqrt{B}$	1.2	0.9	0.7	0.5	0.3
$l^+l^-b\bar{b}$	$S$	1.0	0.9	0.8	0.5	0.3
	$B$	3.6	3.1	2.5	1.8	1.1
	$S/\sqrt{B}$	0.5	0.5	0.5	0.4	0.3
$q\bar{q}b\bar{b}$	$S$	8.1	5.6	3.5	2.5	1.3
	$B$	6800	3600	2800	2300	2000
	$S/\sqrt{B}$	0.10	0.09	0.07	0.05	0.03

TABLE II. Numbers of expected signal and background events in  $1 \text{ fb}^{-1}$  for the high-mass channels.

		Higgs Mass (GeV/c <sup>-1</sup> )						
Channel	Rate	120	130	140	150	160	170	180
$l^\pm l'^\pm l^\mp$	$S$	0.04	0.08	0.11	0.12	0.15	0.10	0.09
	$B$	0.73	0.73	0.73	0.73	0.73	0.73	0.73
	$S/\sqrt{B}$	0.05	0.09	0.13	0.14	0.18	0.12	0.11
$l^+ l^- \nu \bar{\nu}$	$S$	–	–	2.6	2.8	1.5	1.1	1.0
	$B$	–	–	44	30	4.4	2.4	3.8
	$S/\sqrt{B}$			0.39	0.51	0.71	0.71	1.9
$l^\pm l^\mp jj$	$S$	0.1	0.20	0.34	0.53	0.45	0.38	0.29
	$B$	0.85	0.85	0.85	0.85	0.85	0.85	0.85
	$S/\sqrt{B}$	0.11	0.22	0.37	0.57	0.49	0.41	0.31